

Texture analysis of ultra-high coercivity Sm_2Co_7 hot deformation magnets

Qiang Ma(马强), Meishuang Jia(贾美爽), Zhifeng Hu(胡智峰), Ming Yue(岳明), Yanli Liu(刘艳丽), Tongyun Zhao(赵同云), and Baogen Shen(沈保根)

Citation: Chin. Phys. B, 2021, 30 (**4**): 047505. DOI: 10.1088/1674-1056/abe2fc
Journal homepage: http://cpb.iphy.ac.cn; http://iopscience.iop.org/cpb

What follows is a list of articles you may be interested in

Antiferromagnetic interlayer coupling of (111)-oriented $La_{0.67}Sr_{0.33}MnO_3/SrRuO_3$ superlattices

Hui Zhang(张慧), Jing Zhang(张静), Jin-E Zhang(张金娥), Fu-Rong Han(韩福荣), Hai-Lin Huang(黄海林), Jing-Hua Song(宋京华), Bao-Gen Shen(沈保根), Ji-Rong Sun(孙继荣)
Chin. Phys. B, 2019, 28 (**3**): 037501. DOI: 10.1088/1674-1056/28/3/037501

Rare earth permanent magnets prepared by hot deformation process

Ren-Jie Chen(陈仁杰), Ze-Xuan Wang(王泽轩), Xu Tang(唐旭), Wen-Zong Yin(尹文宗), Chao-Xiang Jin(靳朝相), Jin-Yun Ju(剧锦云), Don Lee(李东), A-Ru Yan(闫阿儒)
Chin. Phys. B, 2018, 27 (**11**): 117504. DOI: 10.1088/1674-1056/27/11/117504

Effects of spacer layers on magnetic properties and exchange couplings of Nd-Fe-B/Nd-Ce-Fe-B multilayer films

Ya-Chao Sun(孙亚超), Ming-Gang Zhu(朱明刚), Wei Liu(刘伟), Rui Han(韩瑞), Wen-Chen Zhang(张文臣), Yan-Feng Li(李岩峰), Wei Li(李卫)
Chin. Phys. B, 2017, 26 (**10**): 107501. DOI: 10.1088/1674-1056/26/10/107501

Evolution of structure and magnetic properties in $PrCo_5$ magnet for high energy ball milling in ethanol

Li Zhu-Bai, Lan Jian-Ting, Zhang Xue-Feng, Liu Yan-Li, Li Yong-Feng
Chin. Phys. B, 2015, 24 (**8**): 087501. DOI: 10.1088/1674-1056/24/8/087501

Magnetic and mechanical properties of Ni–Mn–Ga/Fe–Ga ferromagnetic shape memory composite

Tan Chang-Long, Zhang Kun, Tian Xiao-Hua, Cai Wei
Chin. Phys. B, 2015, 24 (**5**): 057502. DOI: 10.1088/1674-1056/24/5/057502

Texture analysis of ultra-high coercivity Sm_2Co_7 hot deformation magnets*

Qiang Ma(马强)[1,2,3], Meishuang Jia(贾美爽)[2], Zhifeng Hu(胡智峰)[2], Ming Yue(岳明)[3], Yanli Liu(刘艳丽)[1,2], Tongyun Zhao(赵同云)[1], and Baogen Shen(沈保根)[1,†]

[1] *State Key Laboratory of Magnetism, Institute of Physics, Chinese Academy of Sciences, Beijing* 100190, *China*
[2] *School of Science, Inner Mongolia University of Science and Technology, Baotou* 014010, *China*
[3] *College of Materials Science and Engineering, Beijing University of Technology, Beijing* 100124, *China*

(Received 15 December 2020; revised manuscript received 20 January 2021; accepted manuscript online 4 February 2021)

Bulk anisotropic Sm_2Co_7 nanocrystalline magnets were successfully prepared by hot deformation process using spark plasma sintering technology. The coercivity of the isotropic Sm_2Co_7 nanocrystalline magnet is 34.76 kOe, further, the ultra-high coercivity of 50.68 kOe is obtained in the anisotropic hot deformed Sm_2Co_7 magnet when the height reduction is 70%, which is much higher than those of the ordinarily produced hot deformed Sm_2Co_7 magnet. X-ray diffraction (XRD) analysis shows that all the samples are Sm_2Co_7 single phase. The investigation by electron backscatter diffraction indicates that increasing the amount of deformation is beneficial to the improvement of the (00l) texture of Sm_2Co_7 magnets. The Sm_2Co_7 nanocrystalline magnet generates a strong *c*-axis crystallographic texture during large deformation process.

Keywords: Sm_2Co_7 magnet, spark plasma sintering, hot deformation, ultra-high coercivity, texture

PACS: 75.47.Np, 75.50.Ww, 75.60.Jk **DOI:** 10.1088/1674-1056/abe2fc

1. Introduction

Sm–Co alloys such as $SmCo_5$, Sm_2Co_{17}, and $SmCo_7$ have been extensively studied for high Curie temperature (T_C) and large magnetocrystalline anisotropy (H_A).[1–7] Sm_2Co_7 is a kind of magnet with great potential for use in high temperature environment due to its large H_A ($>$ 200 kOe) and good phase stability.[8–12] With the development of nanotechnology and the application of spark plasma sintering (SPS) technology in the field of nanocrystalline magnet preparation, the preparation of ultra-high coercivity (H_{cj}) Sm–Co bulk magnets becomes possible.[13] Preparation of Sm–Co alloy magnets by using SPS process can effectively avoid the abnormal growth of crystal grains and provide high coercivity.[14–16] Coercivity and phase stability of Sm_2Co_7 type nanocrystalline magnets have been reported, but few studies have focused on the Sm_2Co_7 anisotropic magnet.[17,18] Magnetic performance of isotropic nanocrystalline Sm_2Co_7 is not high enough due to its low magnetic orientation. Hot deformation process is an effective method to obtain magnetic anisotropy of nanocrystalline magnets. However, strong *c*-axis crystallographic texture has never been reported so far for Sm_2Co_7 nanocrystalline magnet. The present work is aimed to prepare Sm_2Co_7 anisotropic magnet with strong texture by means of hot pressing and hot deformation, and to study the formation mechanism of the texture.

2. Experimental procedures

The Sm_2Co_7 alloy ingots with a stoichiometric ratio 2:7 (at.%) were prepared by induction melting of elemental Sm and Co both with 99.95% purity under the purified argon atmosphere. An excess of 5 wt.% Sm was used to compensate for its losses during the preparation. The ingots were quenched into ribbons at a wheel speed of 30 m/s and then high energy ball milled into amorphous powders. The powders were hot pressed (HP) at 700 °C with a pressure of 450 MPa. In order to obtain anisotropic magnets, the isotropic hot pressed magnets were hot deformed (HD) with height reductions of 70%, 80%, and 90% (named HD70%, HD80%, and HD90%, respectively) at the temperature of 720–750 °C under the pressure of 20–50 kN. The magnetic properties of the samples were measured by vibrating sample magnetometer (VSM). X-ray diffraction (XRD) measurement of the hot pressed and hot deformed samples has been performed by using Co $K\alpha$ radiation. Electron backscatter diffraction (EBSD) was carried out to analyze the orientation and the mechanism of the texture formation. All of the test surfaces of the samples were perpendicular to the direction of pressure.

3. Results and discussion

As shown in Fig. 1, the coercivity H_{cj} of the isotropic Sm_2Co_7 HP magnet is 34.76 kOe, the remanence M_r is

*Project supports by the Science Center of the National Natural Science Foundation of China (Grant No. 52088101), the National Natural Foundation of China (Grant No. 51590880), the Fujian Institute of Innovation, Chinese Academy of Sciences (Grant No. FJCXY18040302), the Key Program of the Chinese Academy of Sciences (Grant No. KJZD-EW-M05-1), and the Natural Science Foundation of Inner Mongolia, China (Grant Nos. 2018LH05006 and 2018LH05011).

†Corresponding author. E-mail: shenbg@iphy.ac.cn

© 2021 Chinese Physical Society and IOP Publishing Ltd

36.23 emu/g, and the maximum energy product $(BH)_{max}$ is 3.76 MGOe. The sample of HD70% exhibits a coercivity as high as 50.68 kOe, which is the highest coercivity that SmCo bulk magnet has ever been reported to possess, and the remanence is 40.05 emu/g. As the die upset level increases to 80%, the coercivity of the magnet still remains 32.32 kOe, and the remanence increases to 48.56 emu/g. For the HD90% sample, the coercivity is drastically reduced to 4.60 kOe, while the remanence is increased to 63.10 emu/g and the maximum energy product is 8.21 MGOe. With the increase of height reduction, the increases of magnetic remanence and magnetic energy product arise from the enhancement of the magnetic anisotropy. The details of the magnetic properties of the Sm_2Co_7 HP and HD magnets are shown in Table 1. The orientation degree of the magnet was calculated by the value of M_r/M_s (M_s is the saturation magnetization at the magnetic field of 70 kOe). It is found that with the increase of the die upset level, the value of M_r/M_s is increased from 82.20% to 94.74%, indicating that the orientation of c-axis of the magnets is optimized.[15]

The result of the Sm_2Co_7 magnet HP sample analyzed using XRD is shown in Fig. 2 by black line. As seen in the pattern, the magnet has a Sm_2Co_7 single phase with a hexagonal Ce_2Ni_7-type structure (PDF# 71-0387) at the room temperature. Figure 2 also shows the XRD patterns of the hot-deformed Sm_2Co_7 magnets. As the die upset level increases, the peak of (00 12) is continually rising while the peak of (116) decreases, which means that the Sm_2Co_7 grains have a preferred orientation during the HD process, resulting in a (00l) texture. The texture strength is quantitatively characterized by the value of $I_{(00\ 12)}/I_{(116)}$. The $I_{(00\ 12)}/I_{(116)}$ of the HP magnet is 0.53, then, with the amount of die upset level increased by 90%, the value of $I_{(00\ 12)}/I_{(116)}$ reaches 6.93, which is 13.08 times higher than that of HP magnet. The strong c-axis texture of the HD90% magnet is the reason for the high value of M_r/M_s and high M_r in Table 1.

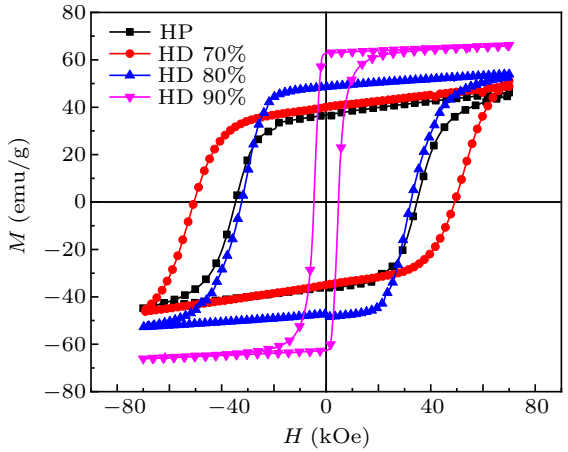


Fig. 1. Hysteresis loop of the Sm_2Co_7 HP and HD magnets.

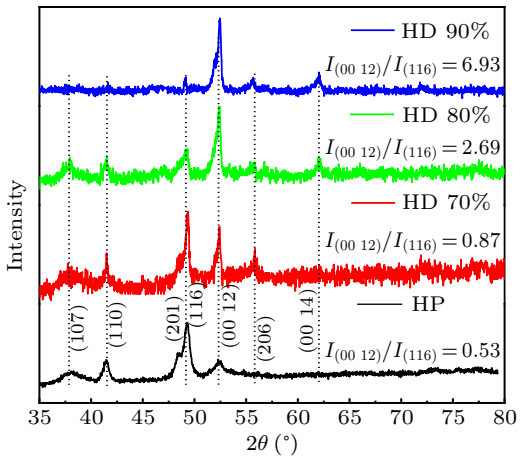


Fig. 2. XRD patterns of the HP and HD Sm_2Co_7 magnets.

Table 1. Magnetic properties of the hot-pressed and hot-deformed Sm_2Co_7 magnets.

Sample	H_{cj} (kOe)	M_r (emu/g)	$M_{s(70\ kOe)}$ (emu/g)	$(BH)_{max}$ (MGOe)	M_r/M_s	ρ (g/cm^3)
HP	34.76	36.23	46.12	3.76	78.56%	8.41
HD 70%	50.68	40.05	48.72	4.47	82.20%	8.52
HD 80%	32.32	48.56	54.46	6.65	89.17%	8.51
HD 90%	4.60	63.10	66.60	8.21	94.74%	8.54

The magnets densities were tested using the Archimedes principle. As shown in Table 1, the density of the magnets after HD process is higher than that of the HP magnet, which indicates that some defects disappear in a long period of high temperature deformation during the HD process. As shown in Fig. 3(a), the grain size of the HD 70% Sm_2Co_7 magnet is about 300 nm, the grain boundaries are clearly visible, and the size of the grain is uniform, which are the reasons for obtaining ultra-high coercivity. In Fig. 3(b), when the amount of the height reduction increases to 80%, the grains grow to 800 nm in size, which decreases the coercivity. The further growth of grains in the HD 90% samples results in the distribution of some micron-sized grains in the magnets, leading to the rapid decline of coercivity.

The orientation texture and microstructure of the HD Sm_2Co_7 magnets were characterized by electron backscatter diffraction scanning (EBSD) analysis. Figures 3(d)–3(f) are EBSD-orientation imaging microscopy (OIM) scans, and figures 3(g)–3(i) are the corresponding inverse pole figures (IPFs) of the Sm_2Co_7 magnets with deformations of the samples under HD70%, HD80%, and HD90%, respectively. In the OIM-EBSD map, the color of a grain specifies its orientation ac-

cording to the color code. As shown in Figs. 3(d)–3(f), there are no unidentified regions in the OIM maps, indicating that all grains are Sm_2Co_7 pure phase. As indicated by the color code, red represents that the grain orientation is parallel to the (001). Comparing the OIMs and their corresponding IPFs of different samples, it can be seen that the increase of deformation is beneficial to the formation of the (001) texture. When the height reduction is 90%, the pole density of the (001) direction is 9.02, which demonstrates that the magnet of HD 90% formed a strong (001) texture, providing a higher remanence for the magnet. Good agreement is obtained among the results of hysteresis loop, XRD, and EBSD.

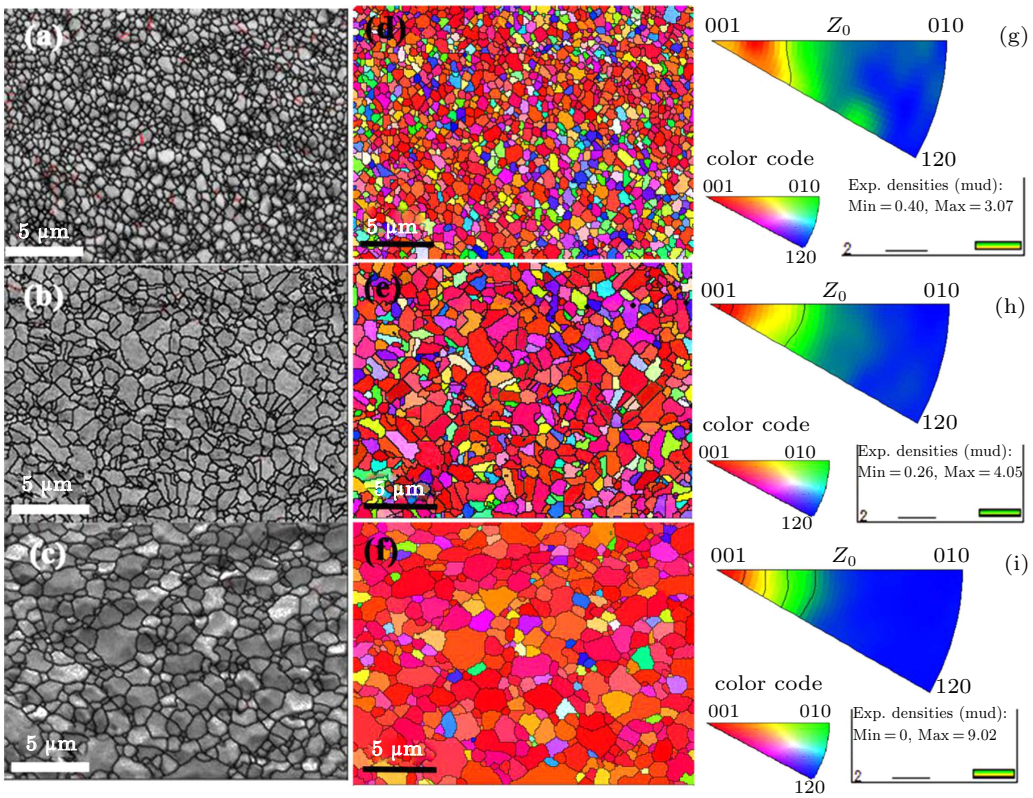


Fig. 3. (a)–(c) Grain size image quality (IQ) map, (d)–(f) OIM-EBSD scan, and (g)–(i) corresponding IPF of the hot deformed Sm_2Co_7 magnets with 70%, 80%, and 90% height reduction, respectively.

To analyze the distribution of the orientation angle of the HD magnets, the distribution of misorientation angles was calculated and illustrated in Fig. 4. The black line in Fig. 4 shows the angular distribution of the orientation difference in the random orientation, and the histograms show the angular distribution of the orientation difference measured by the specimens. The distribution of the grain misorientation angles of the HD magnet is different from the random distribution (black line in Fig. 4), which is due to the continuous evolution of grain orientation during the deformation. The texture is strengthened with the increase of deformation degree, indicating that the concentration of grain misorientation angles is related to the texture. From Fig. 4, it can be seen that the distribution of orientation difference of the HD90% magnet is concentrated around 30°, while the distribution of orientation difference of the HD70% and HD80% magnets is weaker at around 30°. This manifests that during the HD process, the grains tend to form a concentrated orientation relationship while forming the texture, and this orientation relationship is related to the mechanism of the texture formation of the grain rotation and recrystallization.[19–22] The results of XRD, EBSD, and misorientation analysis consistently show that the increase in deformation can promote the formation of (001) texture. Good (001) texture is primary for the permanent magnet materials to improve remanence.

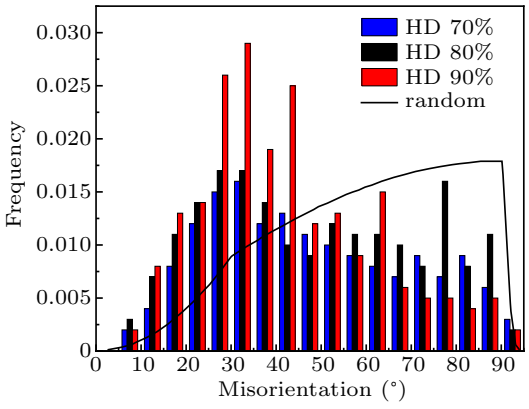


Fig. 4. Distribution of the grain misorientation angles of the Sm_2Co_7 HD magnets.

4. Conclusions and perspectives

In this study, anisotropic Sm_2Co_7 magnets were prepared by using spark plasma sintering and hot deformation techniques. When the height reduction is 70% in the hot-deformed process, an ultra-high coercivity magnet with a coercivity of 50.68 kOe is obtained. The ultra-high coercivity is contributed to the uniform distribution of nano-scale grian size of HD70% samples. The M_r/M_s, XRD, and EBSD OIM analyses are in such a good agreement in proving that the hot deformation process can produce *c*-axis orientation texture of the Sm_2Co_7 magnets, and the larger the deformation amount is, the better the *c*-axis texture of the magnets. And thus, the products of the Sm_2Co_7 magnets are found acquired with higher remanence and magnetic energy. Future work will focus on the mechanism of texture evolution in Sm_2Co_7 hot deformation magnets.

References

[1] Zhang J, Takahashi Y K, Gopalan R and Hono K 2007 *J. Magn. Magn. Mater.* **310** 1

[2] Yue M, Zhang X Y and Liu J P 2017 *Nanoscale* **9** 3674

[3] Skokov K P and Gutflfleisch O 2018 *Scr. Mater.* **154** 289

[4] Liu Y G, Xu L, Wang Q F, Li W and Zhang X Y 2009 *Appl. Phys. Lett.* **9** 172502

[5] Gutflfleisch O, Willard M A, Brück E, Chen C H, Sankar S G and Liu J P 2011 *Adv. Mater.* **42** 821

[6] Yue M, Li C L, Wu Q, Z H Ma, Xu H H and Palaka S 2018 *J. Chem. Eng.* **343** 1

[7] Xu X C, Li Y Q, Ma Z H, Yue M and Zhang D T 2020 *Scripta. Mater.* **178** 34

[8] Nakamura H 2018 *Scr. Mater.* **154** 273

[9] Ma Z H, Liang J M, Ma W, Cong L Y, Wu Q and Yue M 2019 *Nanoscale* **11** 12484

[10] Liu W Q, Zuo J H, Yue M, Lv W C, Zhang D T and Zhang J X 2011 *J. Appl. Phys.* **109** 07a731

[11] Huang M Q, WallaceW E, McHenry M, Chen Q and Ma B M 1998 *J. Appl. Phys.* **83** 6718

[12] Ma Q, Yue M, Lv W C, Zhang H G, Yuan X K, Zhang D T, Zhang X F, Zhang J X and Gao X X 2016 *J. Magn.* **21** 25

[13] Liu S Q 2019 *Chin. Phys. B* **28** 017501

[14] Campos M F, Yonamine T, Fukuhara M, Machado R, Romero S A, Landgraf F J G, Rodrigues D and Missell F P 2007 *J. Appl. Phys.* **101** 09

[15] Yonamine T, Fukuhara M, Machado R and Missell F P 2008 *J. Magn. Magn. Mater.* **320** e77

[16] Ma Q, Yue M, Xu X C, Zhang H G, Zhang D T, Zhang X F and Zhang J X 2018 *AIP. Adv.* **8** 056214

[17] Yue M, Zuo J H, Liu W Q, Lv W C, Zhang D T, Zhang J X, Guo Z H and Li W 2011 *J. Appl. Phys.* **109** 07A711

[18] Fang L, Zhang T, Wang H, Jiang C and Liu J 2018 *J. Magn. Magn. Mater.* **446** 200

[19] Xu W W, Song X Y, Zhang Z X and Liang H N 2013 *Mater. Sci. Eng.* **178** B971

[20] Sakamoto Y, Kojima S, Kojima K, Ohtani T and KuboT 1979 *J. Appl. Phys.* **50** 2355

[21] M. Zhu and Li W 2017 *AIP Advances* **7** 056236

[22] Yuan X K, Yue M, Zhang D T, Jin T N, Zhang Z R, Zuo J H, Zhang J X, Zhu J and Gao X X 2014 *CrystEngComm* **16** 1669